

Wind observations of extreme ion temperature anisotropies in the lunar wake

D. Clack,^{1,2} J. C. Kasper,¹ A. J. Lazarus,¹ J. T. Steinberg,³ and W. M. Farrell⁴

Received 31 July 2003; revised 16 January 2004; accepted 19 February 2004; published 30 March 2004.

[1] We describe Wind observations of two lunar wake encounters which occurred on 12–13 November 1996 and 18 July 2002. The observations were made at downstream distances of around 25 and 15 lunar radii (R_L), respectively. Both encounters occurred prior to the spacecraft entering the lunar shadow; one event took place within the magnetosheath. A characteristic feature of the lunar wake is the presence of two counterstreaming ion beams drawn in from either flank. We find that both ion components exhibit an extreme temperature anisotropy, often with $T_{\perp} \sim 10T_{\parallel}$. The anisotropy is greatest in the central wake region. It appears that the anisotropy arises through the conservation of adiabatic invariants as solar wind plasma expands to fill in the cavity behind the Moon. Despite their large anisotropy, the proton distributions appear stable to the cyclotron instability. Correlated field and flow directional changes show that the wake geometry is dependent upon the prevailing magnetic field orientation. **INDEX TERMS:** 2164 Interplanetary Physics: Solar wind plasma; 2780 Magnetospheric Physics: Solar wind interactions with unmagnetized bodies; 6025 Planetology: Comets and Small Bodies: Interactions with solar wind plasma and fields. **Citation:** Clack, D., J. C. Kasper, A. J. Lazarus, J. T. Steinberg, and W. M. Farrell (2004), Wind observations of extreme ion temperature anisotropies in the lunar wake, *Geophys. Res. Lett.*, 31, L06812, doi:10.1029/2003GL018298.

1. Introduction

[2] Following its launch in 1994, the Wind spacecraft has made many close approaches to the Moon for gravity-assisted orbit changes. During several of these encounters the spacecraft has passed through the lunar plasma wake, a region of low density on the anti-sunward side of the Moon caused by the absorption of solar wind material impinging upon the lunar surface. The lunar wake is an interesting object of study as an example of solar wind interaction with a non-magnetic body, and Wind is the first modern spacecraft with a full range of plasma instrumentation to have encountered the wake.

[3] *Ogilvie et al.* [1996] reported detailed Wind observations of the major plasma features associated with the lunar wake, which include an expanded region of plasma depletion and counterstreaming ion beams [see *Ogilvie et al.*, 1996, Figure 4]. The plasma cavity on the anti-

sunward side of the Moon is replenished by solar wind material but, rather than refilling in a cylindrically symmetric manner, the plasma refilling is restricted by the interplanetary magnetic field. As a result, the wake refills from two flanks. The faster electrons move in first, creating an ambipolar electric field which then draws ions into the wake region [*Samir et al.*, 1983]. Ions from either flank are thus accelerated into and across the cavity along the magnetic field, either speeding up or slowing down dependent upon the prevailing field geometry. Two counterstreaming ion beams of generally unequal density are observed through most of the lunar wake region. As exterior material is drawn into the cavity, a region of low density plasma expands outward behind the Moon — propagating out from the original cavity as a rarefaction wave. In this work, the term ‘wake’ will refer to this expanded region of plasma depletion.

[4] The Faraday Cup instruments of the Solar Wind Experiment (SWE) [*Ogilvie et al.*, 1995] onboard Wind return data on the reduced ion distribution function. In the earlier work of *Ogilvie et al.* [1996], the SWE measurements were fit to isotropic convecting Maxwellian distributions. Presently, following the technique outlined by *Kasper et al.* [2002], and utilizing the Wind MFI measurements of field direction [*Lepping et al.*, 1995], the SWE ion data are fit with convecting bi-Maxwellian distributions. Thus we report here the first analysis of ion thermal anisotropies within the lunar wake. We find that the proton beam distributions evolve into a highly anisotropic state, with $T_{\perp} > T_{\parallel}$, in order to conserve adiabatic invariants. Observations also reveal how the wake geometry responds to changes in the magnetic field orientation.

2. Observations and Results

[5] We describe observations from two separate lunar wake encounters, which we shall term A and B. Event A occurred on 18 July 2002, at a downstream distance of 12–16 lunar radii (R_L). Event B took place over 12–13 November 1996, when Wind was 23–25 R_L downstream. These distances far exceed the crossings made by Explorer 35 near 2 R_L and the previous Wind encounter reported by *Ogilvie et al.* [1996] at 6.5 R_L . The relative trajectory of each crossing with respect to the Moon can be seen in Figure 1. In each case note the offset of the wake from the Moon-Sun line. Hence both crossings were essentially completed before the spacecraft entered the Moon’s optical shadow. For event A, the data suggest that Wind crossed the Earth’s bow shock ~ 1 hour prior to entry into the wake (see Figure 2a), at which time the spacecraft location in GSE coordinates was $(-22.2, 58.6, 2.8)R_E$ (R_E – Earth radii). Thus, the highly-offset wake geometry in this instance was

¹Center for Space Research, Massachusetts Institute of Technology, Cambridge, Massachusetts, USA.

²Now at Swedish Institute of Space Physics, Uppsala, Sweden.

³Los Alamos National Laboratory, Los Alamos, New Mexico, USA.

⁴NASA/Goddard Space Flight Center, Greenbelt, Maryland, USA.

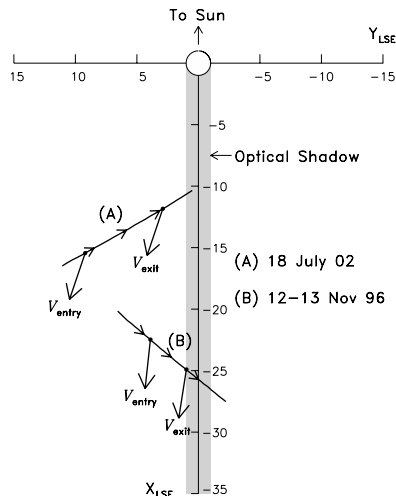


Figure 1. Spacecraft trajectory with respect to the Moon for two lunar wake encounters. LSE refers to a Lunar-centric Solar Ecliptic system of coordinates, with the x -axis directed from the Moon's center toward the Sun, and the y -axis parallel with the ecliptic plane. Arrows show the direction of the solar wind flow at the entry and exit points as Wind passed through the wake.

due to large azimuthal solar wind flows characteristic of the magnetosheath. Since the observed wake signature lasted nearly 3 hours it appears the wake was relatively stable (for the most part — see below), most likely because Wind entered the magnetosheath on its tailward flank where magnetosheath flows are generally less variable. For event B Wind was located in the solar wind at $(47.4, 24.1, 5.0)R_E$. Figure 1 reveals differences in the apparent cross-sectional size of the wake between events. Given the

differing plasma environments in which the events took place (magnetosheath vs. solar wind), contrasts in the observations are to be expected.

[6] Figures 2a and 2b display 6 hours of plasma and magnetic field data encompassing each respective wake crossing. The top four panels show the following proton parameters: number density, n ; perpendicular thermal speed, w_{\perp} ; parallel thermal speed, w_{\parallel} ; and temperature anisotropy, T_{\perp}/T_{\parallel} . The bottom two panels show the magnetic field strength, $|\mathbf{B}|$; the field azimuth angle, ϕ_B (dots); and field elevation angle, θ_B (circles). Field data in event B have been corrected for spin phase errors introduced by the lunar shadow [Owen *et al.*, 1996]. The density profiles clearly show the occurrence of inter-penetrating proton beams streaming in to refill the wake cavity, demonstrating that the characteristic features of the lunar wake remain observable at downstream distances of up to $25 R_L$. (Profiles of other key plasma parameters associated with these events are similar to those presented by Ogilvie *et al.* [1996].) The most central point of each crossing occurs when the beam densities from either flank are roughly equal — note the asymmetric nature of event A. Concurrent with the region of plasma depletion we observe a slight elevation in the magnetic field magnitude [see Owen *et al.*, 1996]. Directional changes in **B** also occur at some of the wake boundaries. Unfortunately, the large values of θ_B seen towards the end of event A inhibit the ability of the Faraday Cups to resolve the two ion beams and prevent us from ascertaining their character. Both events display a similar pattern of anisotropic changes in thermal velocity within the wake: a slight increase in w_{\perp} is accompanied by a dramatic decrease in w_{\parallel} . The cumulative effect of these changes results in an extremely large temperature anisotropy, where the ratio T_{\perp}/T_{\parallel} reaches values of 8 and higher. These values are far in excess of those typically observed in the undis-

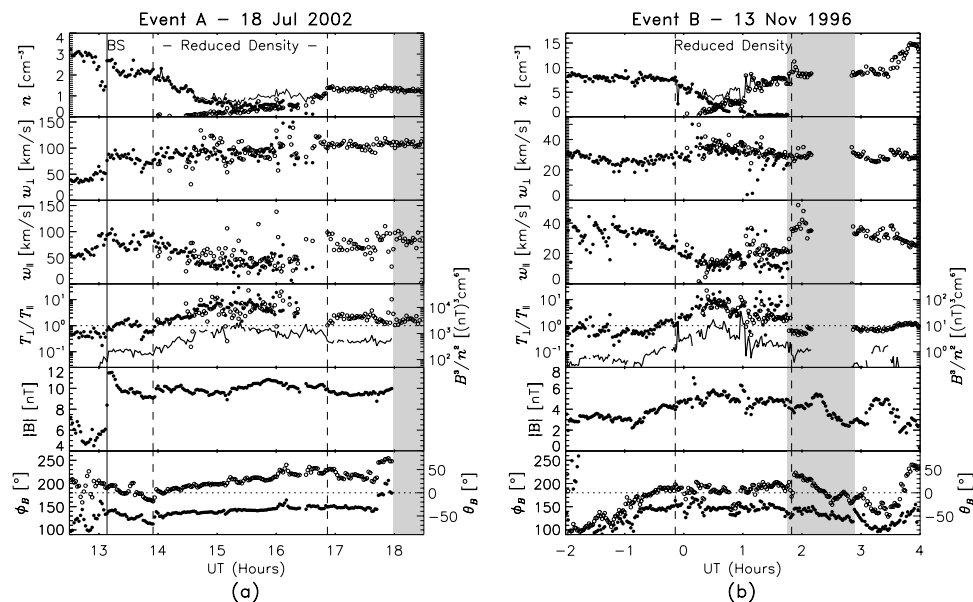


Figure 2. Wind proton and magnetic field data for the two wake encounters as described in the text. Measurements associated with plasma flows originating from the spacecraft entry (exit) side of the wake are indicated by dots (circles), as determined from analysis of flow vectors. Dashed vertical lines mark the intervals of plasma depletion which denote each wake encounter, whilst shaded regions correspond to periods when Wind was in the Moon's shadow. Note the bow shock (BS) crossing in (a) characterised by sharp enhancements in field strength, density and thermal speed.

turbed solar wind [Marsch *et al.*, 1982]. Although relatively large temperature anisotropies are commonly seen in the magnetosheath, it is clear from Figure 2a that the anisotropy in the central wake is considerably greater than that observed in the surrounding magnetosheath plasma. Large temperature anisotropies have been observed in each lunar wake crossing made by Wind that was similarly analysed, 5 events in total occurring at a range of downstream distances between $5 R_L$ and $26 R_L$. We therefore conclude that this anisotropy is an inherent feature of the lunar wake.

[7] The asymmetrical profile of event A in Figure 2a might be related to observable differences in some of the ‘entry’- and ‘exit’-side parameters. In addition to the displayed data we note a 7° change in magnetosheath flow direction, with a decrease in the angle between the flow and magnetic field from 48° at entry to 10° at exit. This suggests that temporal changes in the magnetosheath plasma and magnetic field may have caused the wake to flap or expand/contract in an irregular manner. If the wake topology were to deviate from a simple conical form [e.g., Spreiter *et al.*, 1970] then, coupled with a rotation of \mathbf{B} in the plane perpendicular to the flow, this could also contribute to entry and exit paths of uneven length.

[8] We now turn our attention to identifying the cause of the highly non-thermal ion distributions. The double adiabatic equations of state, first derived by Chew *et al.* [1956], can be written as:

$$\frac{d}{dt} \left(\frac{T_\perp}{B} \right) = 0 \quad (1)$$

$$\frac{d}{dt} \left(\frac{T_\parallel B^2}{n^2} \right) = 0 \quad (2)$$

This description of a plasma is best suited to times when the field is relatively strong, plasma beta ($\beta = nk_B T / (B^2 / 2\mu_0)$) is low, and heat transfer in either the parallel or perpendicular directions is negligible. A simple combination of the invariants contained within the above expressions leads to the following relationship:

$$\frac{T_\perp}{T_\parallel} \propto \frac{B^3}{n^2} \quad (3)$$

Evidence for the validity of equation (3) above with regard to the expansion of plasma downstream of the Moon can be seen in the fourth panels of Figures 2a and 2b, where we have plotted the value of B^3/n^2 (solid line) alongside the temperature ratio T_\perp/T_\parallel (Note: for n here we use total proton density). The correlation within the wake is particularly impressive, with the rise in anisotropy appearing directly proportional to the increase in B^3/n^2 . The main factor in the varying profile of B^3/n^2 is the large change in n (accounting for $\sim 70\%$), with the smaller variation in $|\mathbf{B}|$ being less significant. The exceptional correspondence displayed is testimony that the particle distributions for the two proton beams evolve as collisionless distributions under the influence of relatively strong field without heat transfer.

[9] The agreement between the parameters described above suggests that the highly anisotropic beam distributions are relatively stable. In addition, spectrograms derived from the MFI z -axis sensor (not shown) do not exhibit any sign of increased activity at the low frequencies associated

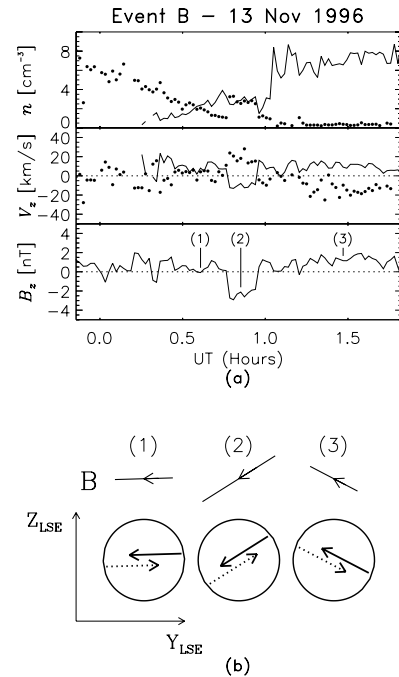


Figure 3. (a) Data for the Nov 1996 wake crossing demonstrating the dependence of plasma observations upon field orientation. Points associated with the entry (exit) side ion beam are shown as dots (solid line). (b) Representation of inferred wake geometry at three distinct points during the encounter.

with ion cyclotron or whistler emission. Thus, there is no evidence of an anisotropy driven instability having been excited to a significant level. As a possible explanation for this, we note the observation that $\beta_\parallel (= (T_\parallel/T) \beta)$ falls to very low values ($\sim 10^{-2}$) within the central wake, ensuring that potential electromagnetic instabilities such as the proton cyclotron anisotropy instability will have a low growth rate. Using results from hybrid simulations [Gary *et al.*, 1994], we can estimate that for $\beta_\parallel = 10^{-2}$ the threshold for the onset of the cyclotron instability would lie near $T_\perp/T_\parallel \sim 7$, close to the values we observe in the central wake. Since the wake density should be much lower nearer the Moon, the ratio B^3/n^2 could potentially be much larger there. Thus, there is greater likelihood of an anisotropy instability having significant growth rate at shorter downstream distances.

[10] Farrell *et al.* [1997] explored the possibility that the counterstreaming ion beams would be susceptible to an electrostatic instability. A 1-D electrostatic simulation [Farrell *et al.*, 1998] suggested that beyond $20 R_L$ such an instability would become sufficiently strong enough (saturated) to disrupt the flow of beaming ions, slowing them down and causing a build-up of ions in the central wake. A simulation with higher phase space resolution led Birch and Chapman [2001] to conclude that the ion beams would be disrupted by electric potentials created by the electron two-stream instability, which occurs on a faster timescale. The solid line indicating total proton density in the top panels of Figure 2 does indeed suggest a build-up of protons in the central wake. However, the second density peak in Figure 2b at 0050 UT may be related to temporal changes in the solar wind (see Figure 3), and it is difficult to discount this as a

factor elsewhere. The topic of possible beam disruption will need to be further explored.

3. Discussion and Conclusions

[11] *Farrell et al.* [1998] discussed whether it is more applicable to characterise the wake structure in terms of ion sonic or magnetosonic processes. Based upon the results of an electrostatic simulation and the first full set of lunar wake measurements made by Wind, *Farrell et al.* [1998] argued the case for an ion sonic wake whose structure would be mainly determined by the ion sonic speed, and where electrostatic processes would play a major role in replenishing the plasma cavity. In such a scenario, the role of the magnetic field orientation is of secondary importance in the interaction. Our observations indicate that within the central wake $\beta \ll 1$ and, as we shall show, the data suggest that the field is directly responsible for determining the wake orientation.

[12] In Figure 3a we focus on the wake crossing of event B. Here we have plotted the proton density together with the components of the velocity and magnetic field in the LSE z -direction. We note an interval near the center of the crossing where the magnetic field turns notably southward for ~ 13 minutes. A distinct rise in the number density of the entry-side beam occurs coincident with this interval, with the density of the exit-side beam also displaying associated changes. During this time the V_z profiles indicate that the beams had opposed flows out of the ecliptic. Correlated changes are observed in V_x and V_y (not shown), and jumps can also be seen in the parallel thermal speed in Figure 2b. The variations in density and thermal speed most likely reflect changes in the ambient solar wind plasma associated with the abrupt change in \mathbf{B} , although beam disruption could also be a factor as discussed earlier. During the latter stage of the crossing the field angle is oriented northward and the beams are seen to flow from the reverse directions. The schematic in Figure 3b attempts to explain the observations by illustrating the inferred wake geometry at three occasions when B_z had distinctly different values. Vectors indicate the relative strength and direction of the magnetic field in the LSE y - z plane, and underneath anti-parallel arrows indicate the flow of ion beams into the wake cavity along field lines. The tilt in field direction is reflected by the opposed north/south flow of each beam, in agreement with the data in Figure 3a.

[13] Our results suggest that the ambient magnetic field has a substantial effect on the direction of the ambipolar electric field and the overall wake geometry. While electrostatic, kinetic processes seem to characterise the wake system, magnetostatic terms also appear to be important (e.g., equations (1) and (2)). A complete picture might be obtained with a multi-dimensional kinetic wake simulation capable of non-parallel \mathbf{E} -ambipolar and \mathbf{B} orientations.

[14] We have conducted the first analysis of ion thermal anisotropy within the lunar wake, and this has revealed that

the characteristic counterstreaming ion beams exhibit inherently nonthermal anisotropic distributions. Upon entry we observe a dramatic cooling of the ions parallel to \mathbf{B} , with w_{\parallel} falling to its lowest values in the central wake region. Consequently, the wake exhibits an extremely large ion temperature anisotropy, often with $T_{\perp} \sim 10T_{\parallel}$. The anisotropy arises through conservation of the double-adiabatic invariants as solar wind plasma expands into the cavity behind the Moon. The apparent stability of the nonthermal ion beam distributions is probably related to the low values of β_{\parallel} seen within the wake. Whilst inconclusive, evidence of increased plasma density in the central wake region is in agreement with the theory [*Farrell et al.*, 1997] that electrostatic processes act to replenish the plasma void. Data show that the plasma flows into the wake are organised around the magnetic field direction.

[15] **Acknowledgments.** The authors are grateful to A. Szabo at NASA/GSFC for providing MFI data. Work at MIT was supported by NASA grant NAG-10915.

References

- Birch, P. C., and S. C. Chapman (2001), Particle-in-cell simulations of the lunar wake with high phase space resolution, *Geophys. Res. Lett.*, *28*, 219.
- Chew, G. F., M. L. Goldberger, and F. E. Low (1956), The Boltzmann equation and the one-fluid hydromagnetic equations in the absence of particle collisions, *Proc. Roy. Soc. London, Ser. A*, *236*, 112.
- Farrell, W. M., M. L. Kaiser, and J. T. Steinberg (1997), Electrostatic instability in the central lunar wake: A process for replenishing the plasma void?, *Geophys. Res. Lett.*, *24*, 1135.
- Farrell, W. M., et al. (1998), A simple simulation of a plasma void: Applications to Wind observations of the lunar wake, *J. Geophys. Res.*, *103*, 23,653.
- Gary, S. P., et al. (1994), The proton cyclotron instability and the anisotropy/B inverse correlation, *J. Geophys. Res.*, *99*, 5903.
- Kasper, J. C., A. J. Lazarus, and S. P. Gary (2002), Wind/SWE observations of firehose constraint on solar wind proton temperature anisotropy, *Geophys. Res. Lett.*, *29*(17), 1839, doi:10.1029/2002GL015128.
- Lepping, R. P., et al. (1995), The Wind magnetic field investigations, *Space Sci. Rev.*, *71*, 207.
- Marsch, E., et al. (1982), Solar wind protons: Three-dimensional velocity distributions and derived plasma parameters measured between 0.3 and 1 AU, *J. Geophys. Res.*, *87*, 52.
- Ogilvie, K. W., et al. (1995), SWE, a comprehensive plasma instrument for the Wind spacecraft, *Space Sci. Rev.*, *71*, 55.
- Ogilvie, K. W., et al. (1996), Observations of the lunar plasma wake from the Wind spacecraft on December 27, 1994, *Geophys. Res. Lett.*, *23*, 1255.
- Owen, C. J., et al. (1996), The lunar wake at 6.8 R_L : Wind magnetic field observations, *Geophys. Res. Lett.*, *23*, 1263.
- Samir, U., K. H. Wright Jr., and N. H. Stone (1983), The expansion of plasma into a vacuum: Basic phenomena and processes and applications to space plasma physics, *Rev. Geophys.*, *21*, 1631.
- Spreiter, J. R., M. C. Marsch, and A. L. Summers (1970), Hydromagnetic aspects of solar wind flow past the moon, *Cosmic Electrodyn.*, *1*, 5.
- D. Clack, Swedish Institute of Space Physics, Box 537, SE-75121 Uppsala, Sweden. (dc@irfu.se)
- W. M. Farrell, NASA/Goddard Space Flight Center, Greenbelt, MD 20771, USA.
- J. C. Kasper and A. J. Lazarus, Center for Space Research, Massachusetts Institute of Technology, Cambridge, MA 02139, USA.
- J. T. Steinberg, Los Alamos National Laboratory, Los Alamos, NM 87545, USA.